Research Article

Nano Research
2023, 16(7): 10412–10419

ISSN 1998-0124 CN 11-5974/O4
https://doi.org/10.1007/s12274-023-5537-x

Stretchable, breathable, and washable epidermal electrodes based on microfoam reinforced ultrathin conductive nanocomposites

Tao Ma[1], Yong Lin[2], Xiaohui Ma[2], Jiaxue Zhang[2], Dongchan Li[1] (✉), and Desheng Kong[2] (✉)

[1] *School of Chemical Engineering and Technology, Hebei University of Technology, Tianjin 300130, China*
[2] *College of Engineering and Applied Sciences, State Key Laboratory of Analytical Chemistry for Life Science, and Jiangsu Key Laboratory of Artificial Functional Materials, Nanjing University, Nanjing 210046, China*

Received: 27 October 2022 / **Revised:** 5 January 2023 / **Accepted:** 30 January 2023

ABSTRACT

Stretchable epidermal electronics allow conformal interactions with the human body for emerging applications in wearable health monitoring and therapy. Stretchable devices are commonly constructed on submillimeter-thick elastomer substrates with limited moisture permeability, thereby leading to unpleasant sensations during long-term attachment. Although the ultrathin elastomer membrane may address this problem, the mechanical robustness is essentially lost for direct manipulations and repetitive uses. Here, we report a stretchable, breathable, and washable epidermal electrode of microfoam reinforced ultrathin conductive nanocomposite (MRUCN). The new architecture involves ultrathin conductive silver nanowire nanocomposite features supported on a porous elastomeric microfoam substrate, which exhibits high moisture permeability for pleasant perceptions during epidermal applications. As-prepared epidermal electrodes show excellent electronic conductivity (8440 $S \cdot cm^{-1}$), high feature resolution (~ 50 μm), decent stretchability, and excellent durability. In addition, the MRUCN retains stable electrical properties during washing to meet the hygiene requirements for repetitive uses. The successful implementation in an integrated electronic patch demonstrates the practical suitability of MRUCN for a broad range of epidermal electronic devices and systems.

KEYWORDS

stretchable conductor, epidermal electronics, breathable conductor, epidermal electrode

1 Introduction

Wearable technology is rapidly evolving towards stretchable forms for seamless integration with the human body [1–4]. The conformal interactions of stretchable devices with soft skins in the context of epidermal electronics establish a stable interface for the acquisition of health-related information and the execution of electrical/thermal stimulations, thereby opening up promising applications in advanced healthcare monitoring [5–7], wearable medical therapy [8, 9], and human–machine interfaces [10–12]. Stretchable electronic devices are commonly constructed over elastomer membranes with limited moisture permeability. Due to stream evaporation from the body for thermoregulation [13, 14], the long-term attachment of non-permeable electronics onto the skin may give rise to unpleasant sensations and even adverse reactions [10, 15, 16]. Soft porous substrates, on the other hand, have been extensively explored as breathable platforms for stretchable electronics including mesh-like membranes [17], elastomer microfoams [18, 19], and stretchy textiles [17, 20, 21]. The interconnected micropores are the enabler of excellent breathability for substantially improved wearing comfort. A variety of nanomaterials have been assembled over the porous substrates to create conductive electrodes with excellent stretchability, including silver nanoparticles [22, 23], silver nanowires (Ag NWs) [12, 24, 25], and thin metallic coatings [26, 27]. In spite of these advancements, device fabrication on these unconventional substrates often requires capital investments in specialized equipment and lab-intensive procedures. An additional issue is the limited patterning resolution of conductive features due to the noncontinuous microstructure of the porous substrates, which cannot fully satisfy the demands for device miniaturizations and complex circuit integrations.

An alternative design utilizes ultrathin elastomer membranes to construct a breathable form of epidermal electronics [28]. Elastomers represent non-ideal barriers for gas molecules due to the presence of rich free volume as the diffusion pathways [29, 30]. The substantially enhanced permeability is thereby accessible at the ultrathin form of the elastomer membrane. In such a platform, the strain engineering approach has been extensively exploited to create stretchable thin film devices in open-mesh designs, simultaneously achieving steam permeable characteristics [10, 28]. An emerging approach harnesses embedded metallic NWs to create breathable nanocomposite electrodes with skin-like deformability [31]. An additional benefit of the ultrathin layout is the low mechanical stiffness for the conformal attachment to the highly textured skins [10, 32, 33]. These desirable attributes are unfortunately at the expense of reduced mechanical robustness. Due to the lack of sufficient stiffness for direct manipulation, the as-prepared ultrathin device requires a carefully designed procedure for transferring onto the human body [28, 34, 35]. In addition, the removal of such a device attached to the skin often demands excessive forces with a high potential to induce structural

Address correspondence to Dongchan Li, dongchanli@hebut.edu.cn; Desheng Kong, dskong@nju.edu.cn

damage [36, 37]. Accordingly, the ultrathin breathable device is commonly regarded as a disposable electronic tattoo for short-term implementations.

To overcome these challenges, a microfoam reinforced ultrathin conductive nanocomposite (MRUCN) is reported in this study as a new architecture to combine the best of existing designs of stretchable and breathable epidermal electronics. Ag NWs embedded in ultrathin elastomer membranes form compliant nanocomposite electrodes with inherent gas permeability. An elastomeric microfoam serves as a soft and permeable substrate to achieve convenient manipulations and repetitive uses. A screen-printing-based approach is established for the scalable patterning of the nanocomposite electrodes, which exhibit excellent conductivity (8440 $S \cdot cm^{-1}$), high feature resolution (~ 50 μm), decent stretchability (up to 80%), and electromechanical durability. The overall architecture of the ultrathin electrode on porous microfoam ensures high steam permeability above 11.4 $g \cdot h^{-1} \cdot m^{-2}$ for pleasant perceptions during epidermal applications. The MRUCN retains stable electrical properties after multiple washing cycles to satisfy the hygiene requirements for long-term implementations. The practical suitability is demonstrated by the successful fabrication of an integrated electronic patch for epidermal sensing and stimulations. The developments reported here provide a robust material platform to construct breathable forms of epidermal electronics.

2 Experimental

2.1 Materials and synthesis

The thermoplastic elastomer of hydrogenated styrene-ethylene-butylene-styrene (SEBS, Tuftec H1052) was obtained from Asahi Kasei Corporation. All chemical reagents were purchased from Shanghai Macklin Biochemical Co., Ltd. without further purification. Silver nanowires were synthesized by using a polyol-reduction method. Briefly, 3 g polyvinylpyrrolidone (PVP) and 2.5 g $AgNO_3$ were thoroughly dissolved in 600 mL ethylene glycol. After the addition of 900 μL 88 mM $CuCl_2$ solution, the mixture in a flask was heated to 160 °C and then held for 70 min. After the reaction, as-synthesized Ag NWs were repeatedly washed with isopropanol to remove excessive PVP. Ag NWs were then redispersed in isopropanol at a concentration of 5 $mg \cdot mL^{-1}$. As-synthesized Ag NWs had a characteristic length of 86.5 ± 1.1 μm according to Fig. S1 in the Electronic Supplementary Material (ESM). Salicylic acid microrods of ~ 15 μm in length and ~ 6 μm in width were synthesized in an antisolvent crystallization process.

2.2 Preparation and patterning of stretchable electrodes

As-synthesized Ag NWs were spray-deposited onto an octadecyl trichlorosilane (OTS)-modified glass wafer. The subsequent screen-printing procedure generated H-SEBS elastomer patterns from its 25% (w/v) solution in toluene as an effective etching mask. A manual screen printer from Zhuhai Kaivo Electronic Co., Ltd. was employed for the printing process by using a 300-mesh nylon screen. The printed features were dried at 60 °C for 20 min in an oven. The exposed Ag NWs were removed in a mixed aqueous etchant of 15% (w/v) hydrogen peroxide and 14% (w/v) ammonium hydroxide. After thorough rinsing in deionized water, the entire glass wafer was annealed at 120 °C for 20 min to improve the adhesion of Ag NWs to the elastomer. In the meanwhile, salicylic acid microrods and an H-SEBS solution (17% (w/w) in toluene) were thoroughly mixed in a 3:1 weight ratio by stirred bead milling at 2000 rpm for 2 h in an FS400-ST laboratory dissolver from Shanghai Li Chen Co., Ltd. The viscous mixture was drop-cast onto an OTS-modified glass wafer and then naturally dried to yield a composite substrate. As regards the pattern transfer, the Ag NW electrodes were thermally bonded to the composite substrate under the optimized processing parameters in an automatic vacuum laminator (temperature = 110 °C, pressure = 0.07 kPa, and duration = 3 min). The sample was readily peeled off from the OTS-modified non-sticky glass wafer and then submerged in ethanol for 2 h to dissolve the embedded salicylic acid microrods. Conductive Ag NW electrode on the elastomer microfoam was obtained after drying at 60 °C for 10 min.

2.3 Material characterizations

Optical microscopy images and optical surface topographical images were captured by using a Keyence VK-X1000 confocal laser scanning microscope. Scanning electron microscopy (SEM) images were obtained with a Zeiss Model Ultra55 field-emission scanning electron microscope. Optical images and videos were acquired with a Fujifilm X-T10 camera. The electrical resistance was measured under a four-point probe configuration by using a Keithley 2110 digital multimeter. All tensile strains were applied by using a homemade motorized translation stage. Stream permeability tests were evaluated according to the guidelines of the ASTM E96-95 standard. Briefly, a glass jar filled with deionized water was sealed by the sample and stored in an environmental chamber (relative humidity = 50% ± 2%). The glass jar was periodically weighed by an analytical balance (± 0.1 mg). Long-term storage stability was evaluated by placing the sample in an environmental chamber with controlled humidity levels. The resistance was recorded daily for 14 consecutive days. The washing protocol was adopted from previous reports to evaluate candidate materials in a lab setting [38, 39]. Briefly, the sample (3 cm × 1 cm × 0.8 mm) was immersed in tap water, containing 10% (w/v) Blue Moon laundry detergent, if necessary, with the edge attached to the rim of a beaker. The sample underwent a simulated laundry cycle involving vigorous stirring at 1000 rpm for 1 h. After washing with deionized water, the sample was thoroughly dried at 60 °C for 30 min.

2.4 Fabrication and operation of multifunctional electronic patch

A multifunctional device was prepared to comprise a biopotential sensor, an electrical stimulator, a hydration sensor, and interconnects. An additional 10 μm-thick porous microfoam was attached to the interconnect regions for encapsulation. A flexible Cu-clad polyimide connector was bonded to the electronic patch as the interface with the external recording equipment. The patch was sewn onto the skin-tight sleeve to ensure conformal contact with human skin. Written consent was obtained from all volunteers participated in this study. The electronic patch was attached to the forearm with sensing electrodes located at the right flexor carpi radialis. Skin–electrode contact impedance was measured using a GW Instek LCR meter (LCR-6300). The raw EMG signals were conditioned by an Intan RHD2000 amplifier and then sampled at 2 kHz by using an Intan RHD USB interface board. A Camry EH101 digital hand dynamometer was employed as an indicator to achieve a constant grip force. The impedance of the hydration sensor was measured by an LCR meter at 120 kHz to minimize the contribution of skin–electrode contact impedance. An M-6602 skin moisture sensor (Fu Heng Tong Technology Co., Ltd.) was utilized for calibration. A Keithley 2634B digital source meter was employed to generate monophasic square voltage pulses for electrical stimulation (duration = 4 ms, amplitude = 5 V, frequency = 10 Hz).

3 Results and discussion

The overall design of MRUCN is illustrated by the exploded architecture diagram in the inset of Fig. 1(a). An ultrathin nanocomposite electrode comprising a Ag NW percolation network in a SEBS membrane exhibits inherent stream permeability. SEBS microfoam serves as a porous substrate to accommodate the ultrathin electrode. MRUCN represents an attractive platform for epidermal electrodes by combining excellent breathability for comfortable perceptions and mechanical deformability for conformal attachment. The ultrathin nanocomposite membrane alone is a substrate-free epidermal electrode in a vulnerable construction, which is easily folded or torn apart upon detachment from the skin (see Fig. S2 in the ESM). In contrast, a representative MRUCN is prepared with a conductive word pattern of "SOFT", as shown in Fig. 1(b). The soft and stretchy electrode is sufficiently robust to withstand various mechanical manipulations including folding, twisting, and stretching. Accordingly, MRUCN provides a permeable and stretchable architecture for epidermal electronics without sacrificing mechanical robustness.

Figure 2(a) schematically illustrates the overall fabrication process to create the stretchable and breathable epidermal electrodes. Briefly, as-synthesized Ag NWs are spray-deposited on a non-sticky wafer and then partially protected by screen-printed elastomer features. Conductive features are formed by removing exposed Ag NWs in a chemical etching bath [40]. In the meanwhile, salicylic acid microrods are synthesized through an antisolvent method as the porogen [19, 41]. The salicylic acid microrods are thoroughly dispersed into SEBS elastomer to create a composite substrate. The conductive nanocomposite feature is attached to the SEBS/salicylic acid composite substrate inside a vacuum laminator. The combined heat and pressure promote the interfacial diffusion of the thermoplastic elastomer to form a robust bond [40, 42]. The entire sample is subsequently rinsed in ethanol to dissolve the embedded salicylic acid microrods, thereby forming the porous microstructure to complete the fabrication process. In both dry and wet conditions, the tough interfacial adhesion has been achieved under the optimized lamination conditions, as confirmed by 180-degree peel tests in Fig. S3 in the ESM [43].

In Fig. 2(b), a butterfly-shaped nanocomposite is prepared by this process to demonstrate the scalable fabrication of arbitrary features. As-prepared nanocomposite exhibits an excellent conductivity of ~ 8400 S·cm^{-1}. An array of line-shaped electrodes is created to show the accessible feature resolution up to ~ 50 μm (see Fig. 2(b)). The zigzag edge originating from the pixelated screen is open to further improvement by increasing the mesh count [44]. In Fig. 2(c), the SEM image reveals the microstructure of the nanocomposite electrode composed of randomly oriented Ag NWs embedded in the elastomer membrane. The typical thickness of the ultrathin membrane is determined as 4.7 μm (see Fig. S4 in the ESM). As illustrated in Fig. S5 in the ESM, the nanocomposite electrode shows excellent environmental stability for long-term storage at different humidity levels likely due to the Ag NW network fully embedded in the elastomer matrix. The SEBS microfoam contains interconnected micropores in tens of micrometers (see Fig. 2(d)). In Fig. S6 in the ESM, the uniaxial tensile stress–strain curve reveals the compliant nature of the SEBS microfoam with a large fracture strain of 435%. In comparison with the solid elastomer, the microfoam exhibits a lowered modulus of 0.39 MPa which is comparable to the human skin [45].

As regards the stretchability, the resistance of MRUCN as a function of the tensile strain is shown in Fig. 2(e). Specifically, the normalized resistance is 14 at 50% strain, and 41 at 80% strain. The limited increase of the resistance is ascribed to structural damages of inter-nanowire junctions upon stretching [46–48]. For Ag NWs directly transferred to SEBS microform, the electrode resistance demonstrates rapid increases in response to tensile deformations, as shown in Fig. S7 in the ESM. The degraded electrical properties are primarily associated with the fractures of suspended Ag NWs at the micropores. The MRUCN mitigates such a failure mechanism for improved stretchability by fully embedding Ag NWs in the elastomer membrane. In addition, the area loading of the Ag NWs exhibits pronounced influences on the stretchability of the nanocomposite electrodes as illustrated in Fig. S8 in the ESM. Initially, the sensitivity to tensile strain is suppressed by loading additional silver nanowires to densify the percolation network [49]. The excessive loading, on the other hand, gives rise to mechanical stiffening effects and degraded stretchability on the nanocomposite [49]. The optimal

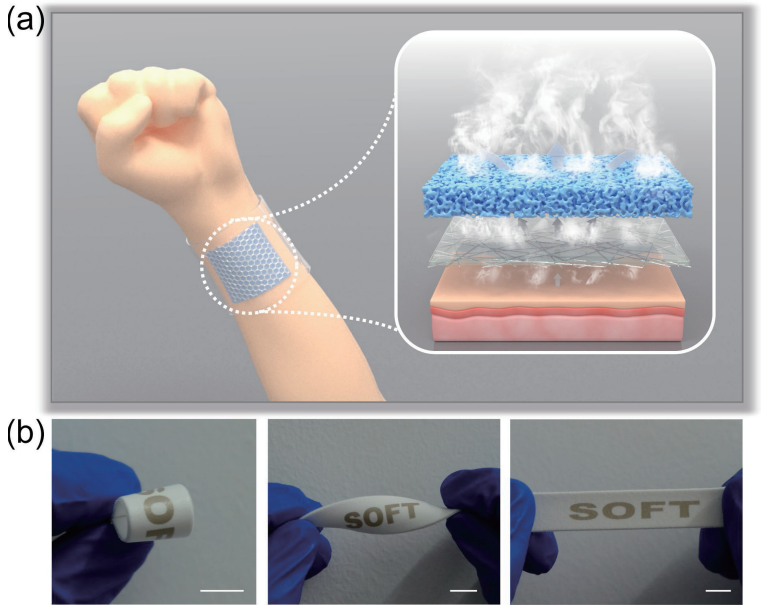

Figure 1 Stretchable and breathable electrode of MRUCNs. (a) Schematic illustrating MRUCN as a breathable epidermal electrode comprising Ag NW and SEBS composite membranes supported on SEBS microfoams. (b) Optical images of stretchable and breathable electrodes operated under bent, twisted, and stretched states. Scale bars: 1 cm.

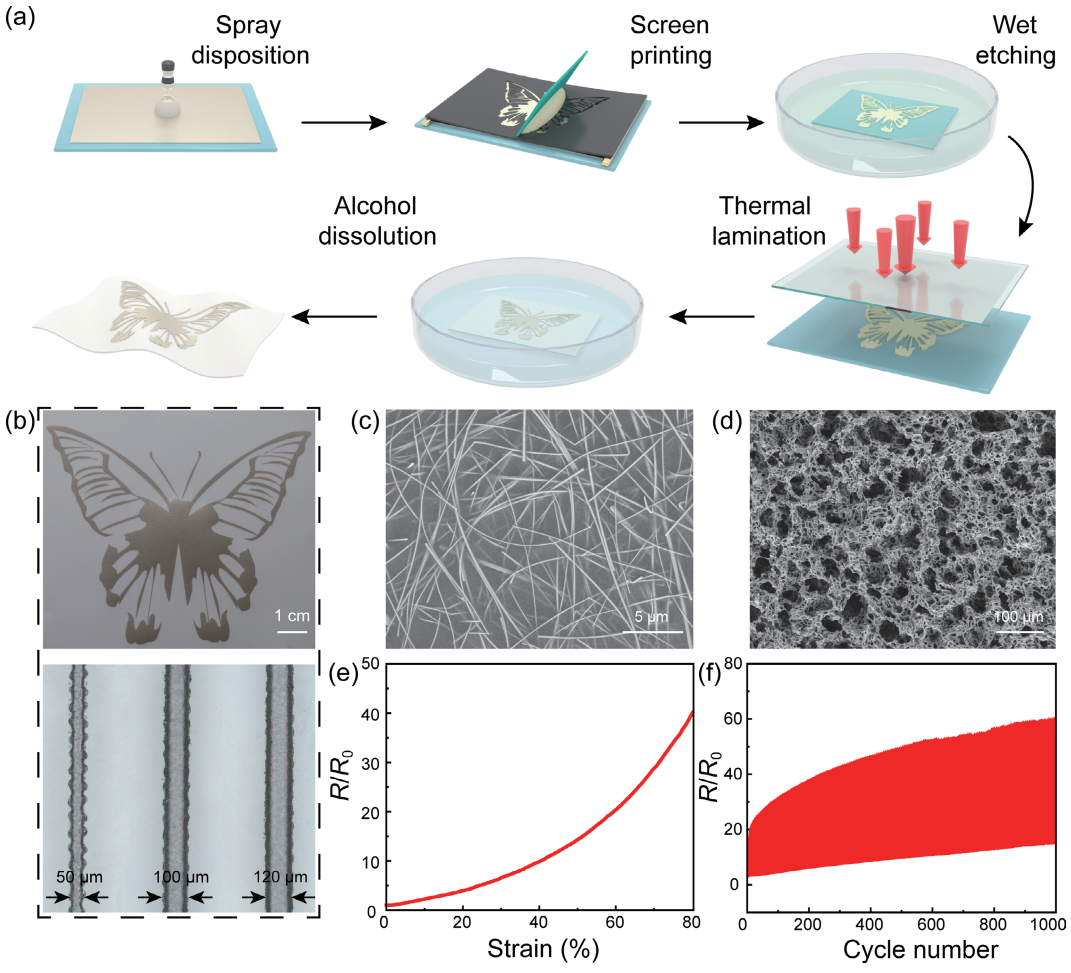

Figure 2 Preparation and characterizations of MRUCN. (a) Schematic illustration of the fabrication process to create patterned Ag NWs as stretchable and breathable electrodes. (b) Optical image of a butterfly-shaped pattern of the Ag NW electrode on a SEBS microfoam (top) and the as-prepared Ag NW electrode to reveal the pattern morphology and feature solution (bottom). (c) SEM image of Ag NWs embedded in SEBS elastomer. (d) SEM image of SEBS microfoam. (e) Normalized resistance of the stretchable electrode as a function of uniaxial tensile strain. (f) Evolution in the resistance of stretchable electrode over 1000 stretch–relaxation cycles to 40% strain.

performance achieved at 0.91 mg·cm^{-2} is therefore selected for the subsequent studies. The nanocomposite electrode is further examined by the tensile fatigue test involving 1000 stretch/release cycles to 40% strain. In Fig. 2(f), the resistance has an irreversible change of 14.7 times throughout the test, as compared competitively against previous reports [50, 51]. The resistance at 40% strain shows initially rapid increases and subsequent gradual saturations. The suppression of uncontrolled conductivity degradations suggests the excellent mechanical durability of the MRUCN for practical applications.

A permeable design is essential for the wearing comfort of epidermal electronics. In Fig. 3(a), the porous SEBS microfoam exhibits high steam permeability of 18.2 g·h^{-1}·m^{-2} due to the plenty of interconnecting channels for gas transmission. The value is comparable to regular textiles for daily garments (19.2 g·h^{-1}·m^{-2}). In contrast, the 100 μm-thick SEBS elastomer is commonly regarded as a non-breathable substrate with a low permeability of 1.1 g·h^{-1}·m^{-2}, thereby substantially blocking the transepidermal water loss of the human body (~ 5–10 g·h^{-1}·m^{-2}) [14]. The permeability is readily improved by thinning down the elastomer to accelerate the molecular diffusion, as shown in Fig. S9 in the ESM. High steam permeability of 11.6 g·h^{-1}·m^{-2} is achieved in 5 μm-thick SEBS membrane to satisfy the thermal regulation requirement for conformable perceptions. Notice that a 4.7 μm-thick nanocomposite is created by the screen-printing-based patterning process to match such a design consideration (see Fig. S4 in the ESM). The MRUCN inherits the breathable characteristics of the ultrathin membrane and the porous microfoam, which exhibits excellent permeability of 11.4 g·h^{-1}·m^{-2} to satisfy the physiological demands. In practice, the nanocomposite electrode is typically in special patterns without full coverage over the microfoam. In Fig. 3(b), the steam permeability is directly correlated with the area fraction in terms of 17.7 g·h^{-1}·m^{-2} at 25%, 16.8 g·h^{-1}·m^{-2} at 50%, 16.0 g·h^{-1}·m^{-2} at 75%, and 11.4 g·h^{-1}·m^{-2} at 100%. The hollow space of the epidermal electrode pattern may further boost the permeable characteristics during practical applications.

Washability is an essential hygiene requirement of epidermal electrodes for long-term applications. A representative MRUCN with a bowtie-shaped pattern is covered with dirt stains after regular usage, as shown in Fig. 3(c). MRUCN is readily cleaned by washing without any obvious damage to the conductive pattern. The change in the electrical property is further evaluated by simulated washing tests in the lab environment [38, 39], as shown in Fig. 3(d). The noticeable drop in resistance upon washing is attributed to the reduced junction resistance between Ag NWs by partially removing the PVP surfactant [39]. The resistance becomes stabilized after three laundry cycles due to the preservation of Ag NWs with strong bonding to the substrate (see Fig. S10 in the ESM). The fairly stable resistance suggests the excellent washability of MRUNE to enable repetitive uses beyond disposable devices.

MRUCN exhibits excellent electronic conductivity, high patterning resolution, decent stretchability, and washability. A

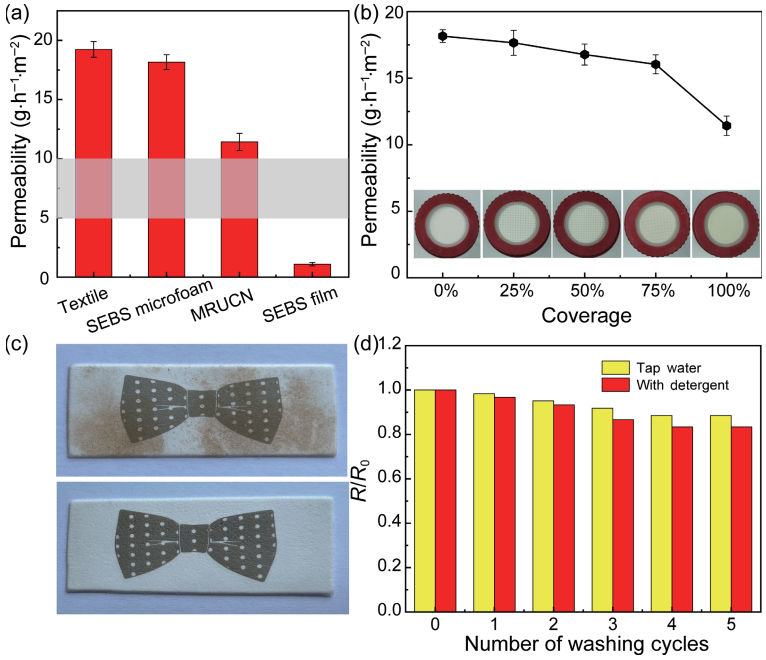

Figure 3 MRUCN for breathability and washability. (a) Steam permeability for a conventional textile, SEBS microfoam, MRUCN, and SEBS film. (b) Steam permeability for patterned electrodes of different coverage. Inset: optical images showing the patterned electrodes. (c) Optical images showing the washability of a bowtie-shaped electrode on SEBS microfoam. (d) Normalized resistance as a function of washing cycles.

summary of stretchable and breathable conductors is provided in Table S1 in the ESM for comparisons. The excellent performances of MRUCN are largely associated with its unique architecture. The continuous nanocomposite layer achieves excellent conductivity with a high-density Ag NW percolation network. The ultrathin forms of elastomer membranes enhance breathability and allow scalable fabrication into delicate features. The microfoam is an essential permeable support for mechanical robustness and repetitive washability. MRUCN combines the attributes of conventional porous conductors and ultrathin membrane conductors, which represent an attractive platform for stretchable and breathable electronics.

Encouraged by the above results, we employ MRUCN to build functional epidermal electronic devices. An integrated electronic patch is created with multiple components including a biopotential sensor, an electrical stimulator, and a hydration sensor (see Fig. 4(a)). An as-prepared patch is sewn onto a compression arm sleeve to create an electronic wearable. The sung fit of the arm sleeve allows the conformal attachment of the epidermal electronics onto the forearm, as shown in Fig. 4(b). The seamless interactions of epidermal electrodes with the skin give rise to low contact impedance comparable to commercial Ag/AgCl gel electrodes (see Fig. 4(c)). At the right extensor carpi radialis, the EMG waveforms are captured by the biopotential sensor corresponding to hand open and closed gestures with a constant grasp force of ~ 200 N (see Fig. 4(d)). Specifically, the signal-to-noise ratio (SNR) is 16.6 dB for nanocomposite electrodes and 18.4 dB for standard Ag/AgCl gel electrodes. In Fig. 4(e), the EMG signal amplitude is directly correlated with the grasping forces, thereby establishing a force-sensitive human–machine interface [52]. In addition, skin hydration is a physiological indicator of skin quality and health conditions [53, 54]. In Fig. 4(f), the hydration sensor utilizes the interdigitated electrode to measure the skin impedance at different hydration states. The impedance amplitude is lowered by increasing the hydration level due to the improved ion conductivity [55] (see Fig. S11 in the ESM). In regular indoor conditions, the skin hydration level is fairly stable as illustrated in Fig. 4(g). A commercial toner effectively raises the skin hydration, followed by a natural decay over time to reach a steady value in ~ 6 min. In addition to the epidermal acquisition of health information, the electrical stimulator supplied monophasic square voltage pulses to the skin for neuromuscular responses [55]. In Fig. 4(h), the perception threshold shows an inverse correlation with the stimulation frequency due to the reduced contact impedance [56]. A subconscious electrical stimulation provides an attractive approach to alleviating pain and restoring physical function [57, 58]. In practice, the simultaneously acquired waveform of the biopotential sensor is well correlated with the stimulation pulses as illustrated in Fig. 4(i), which allows facile monitoring of the implementations of the subconscious therapeutic protocols.

4 Conclusions

In summary, we have introduced the design and fabrication of MRUCN for a stretchable and breathable form of epidermal electronics. In this architecture, the ultrathin Ag NW nanocomposite is supported on a soft and porous substrate of SEBS elastomer microfoam, thereby demonstrating robust properties for direct manipulations including bending, twisting, and stretching. A screen-printing approach allows the scalable fabrication of ultrathin silver nanowire nanocomposite electrodes with excellent conductivity (8440 S·cm^{-1}), high feature resolution (~ 50 μm), decent stretchability (up to 80%), and electromechanical durability. The overall architecture exhibits high steam permeability for breathable perceptions during epidermal applications. The long-term usability is further supported by the robust electrical properties to withstand washing procedures. A multifunctional electronic patch utilizes MRUCN to achieve seamless integration with the human body for epidermal sensing and stimulations. The MRUCN effectively combines the attributes of existing permeable electrode designs to open up an attractive platform for next-generation wearable electronics in terms of stretchability, breathability, washability, and skin conformability.

Acknowledgements

This work was supported by Key Research and Development

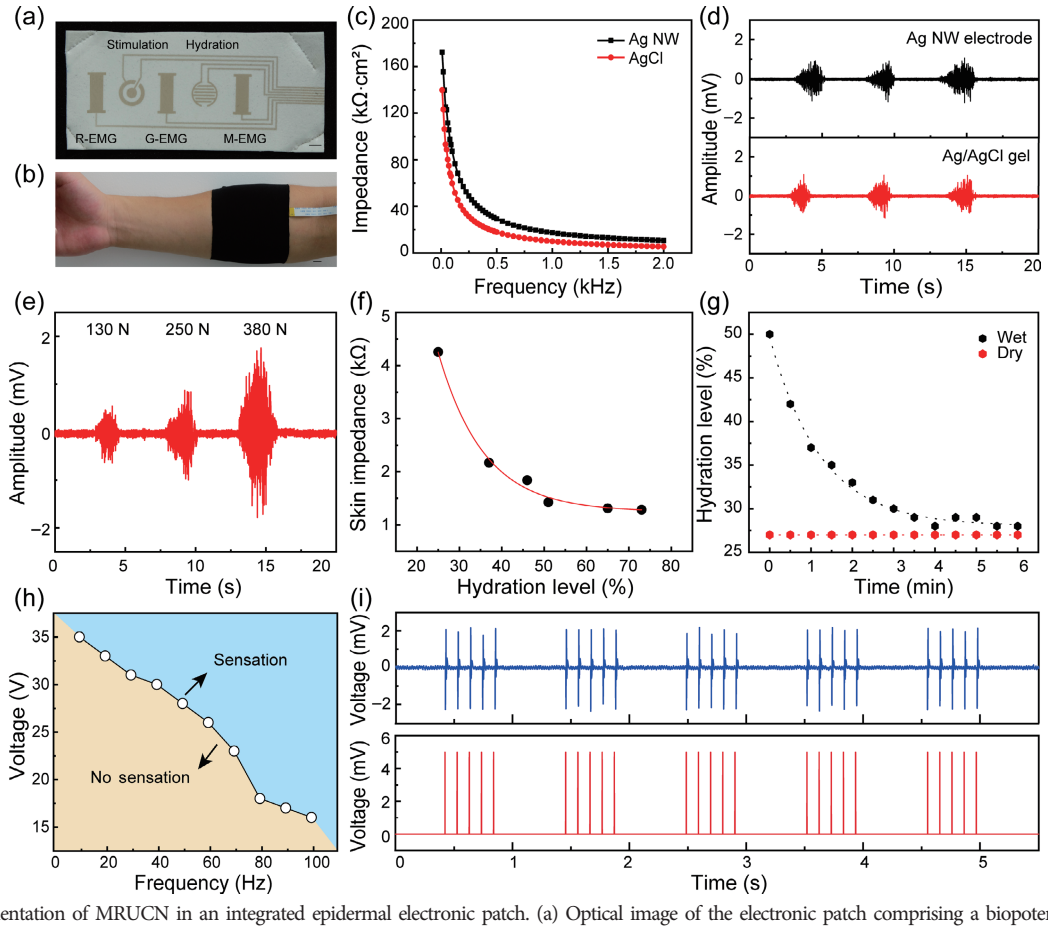

Figure 4 Implementation of MRUCN in an integrated epidermal electronic patch. (a) Optical image of the electronic patch comprising a biopotential sensor, an electrical stimulator, and a hydration sensor. Scale bars: 1 cm. (b) Conformal attachment of a multifunctional electronic patch on the forearm by using a skin-tight arm sleeve. Scale bars: 1 cm. (c) Skin–electrode contact impedance versus frequency for Ag NW electrodes and commercial Ag/AgCl gel electrodes. (d) EMG waveforms of repeated hand opening and closing gestures acquired by using Ag NW electrodes (top) and Ag/AgCl gel electrodes (bottom). (e) EMG waveforms recorded with Ag NW electrodes for hand closing gestures with different grasp forces. (f) Skin impedance versus skin hydration level. (g) Evolution of skin hydration under dry and wet conditions. (h) Voltage threshold for perception as a function of stimulation frequency. (i) EMG waveforms (top) recorded during electrical stimulations with monophasic voltage pulses (bottom).

Program of Jiangsu Provincial Department of Science and Technology of China (No. BE2019002), Key Research and Development Program of Hebei Provence (No. 19251804D), and High-Level Entrepreneurial and Innovative Talents Program of Jiangsu Province.

Electronic Supplementary Material: Supplementary material (including additional characterizations of as-synthesized Ag NWs, free-standing nanocomposite membrane, and washed nanocomposite, measurements of the peeling strength, surface topographic image of the screen-printed membrane, long-term storage stability, stress–strain curve of SEBS microfoam, stretchability of Ag NWs directly transferred to SEBS microfoam, stretchability of MRUCN at different Ag NW mass loadings, stream permeability of SEBS membranes with different thicknesses, impedance spectra of the hydration sensor at different skin hydration levels) is available in the online version of this article at https://doi.org/10.1007/s12274-023-5537-x.

References

[1] Rogers, J. A.; Someya, T.; Huang, Y. G. Materials and mechanics for stretchable electronics. *Science* **2010**, *327*, 1603–1607.

[2] Wang, S. H.; Oh, J. Y.; Xu, J.; Tran, H.; Bao, Z. N. Skin-inspired electronics: An emerging paradigm. *Acc. Chem. Res.* **2018**, *51*, 1033–1045.

[3] Chortos, A.; Liu, J.; Bao, Z. N. Pursuing prosthetic electronic skin. *Nat. Mater* **2016**, *15*, 937–950.

[4] Choi, S.; Lee, H.; Ghaffari, R.; Hyeon, T.; Kim, D. H. Recent advances in flexible and stretchable bio-electronic devices integrated with nanomaterials. *Adv. Mater.* **2016**, *28*, 4203–4218.

[5] Chung, H. U.; Kim, B. H.; Lee, J. Y.; Lee, J.; Xie, Z. Q.; Ibler, E. M.; Lee, K.; Banks, A.; Jeong, J. Y.; Kim, J. et al. Binodal, wireless epidermal electronic systems with in-sensor analytics for neonatal intensive care. *Science* **2019**, *363*, eaau0780.

[6] Wang, X. W.; Gu, Y.; Xiong, Z. P.; Cui, Z.; Zhang, T. Silk-molded flexible, ultrasensitive, and highly stable electronic skin for monitoring human physiological signals. *Adv. Mater.* **2014**, *26*, 1336–1342.

[7] Wang, S. L.; Nie, Y. Y.; Zhu, H. Y.; Xu, Y. R.; Cao, S. T.; Zhang, J. X.; Li, Y. Y.; Wang, J. H.; Ning, X. H.; Kong, D. S. Intrinsically stretchable electronics with ultrahigh deformability to monitor dynamically moving organs. *Sci. Adv.* **2022**, *8*, eabl5511.

[8] Yao, G.; Mo, X. Y.; Yin, C. H.; Lou, W. B.; Wang, Q.; Huang, S. R.; Mao, L. N.; Chen, S. H.; Zhao, K. N.; Pan, T. S. et al. A programmable and skin temperature-activated electromechanical synergistic dressing for effective wound healing. *Sci. Adv.* **2022**, *8*, eabl8379.

[9] Bang, S.; Tahk, D.; Choi, Y. H.; Lee, S.; Lim, J.; Lee, S. R.; Kim, B. S.; Kim, H. N.; Hwang, N. S.; Jeon, N. L. 3D microphysiological system-inspired scalable vascularized tissue constructs for regenerative medicine (Adv. Funct. Mater. 1/2022). *Adv. Funct. Mater.* **2022**, *32*, 2270001.

[10] Jeong, J. W.; Yeo, W. H.; Akhtar, A.; Norton, J. J. S.; Kwack, Y. J.; Li, S.; Jung, S. Y.; Su, Y. W.; Lee, W.; Xia, J. et al. Materials and optimized designs for human–machine interfaces via epidermal electronics. *Adv. Mater.* **2013**, *25*, 6839–6846.

[11] Wang, M.; Yan, Z.; Wang, T.; Cai, P. Q.; Gao, S. Y.; Zeng, Y.; Wan, C. J.; Wang, H.; Pan, L.; Yu, J. C. et al. Gesture recognition using a

bioinspired learning architecture that integrates visual data with somatosensory data from stretchable sensors. *Nat. Electron.* **2020**, *3*, 563–570.

[12] Zhao, H. X.; Zhou, Y. L.; Cao, S. T.; Wang, Y. F.; Zhang, J. X.; Feng, S. X.; Wang, J. C.; Li, D. C.; Kong, D. S. Ultrastretchable and washable conductive microtextiles by coassembly of silver nanowires and elastomeric microfibers for epidermal human–machine interfaces. *ACS Mater. Lett.* **2021**, *3*, 912–920.

[13] Frederick Frasch, H.; Bunge, A. L. The transient dermal exposure II: Post-exposure absorption and evaporation of volatile compounds. *J. Pharm. Sci.* **2015**, *104*, 1499–1507.

[14] Pinnagoda, J.; Tupkek, R. A.; Agner, T.; Serup, J. Guidelines for transepidermal water loss (TEWL) measurement: A report from the standardization group of the European society of contact dermatitis. *Contact Dermatitis* **1990**, *22*, 164–178.

[15] Ma, Z. J.; Huang, Q. Y.; Xu, Q.; Zhuang, Q. N.; Zhao, X.; Yang, Y. H.; Qiu, H.; Yang, Z. L.; Wang, C.; Chai, Y. et al. Permeable superelastic liquid-metal fibre mat enables biocompatible and monolithic stretchable electronics. *Nat. Mater.* **2021**, *20*, 859–868.

[16] Wang, Y. F.; Wang, J.; Cao, S. T.; Kong, D. S. A stretchable and breathable form of epidermal device based on elastomeric nanofibre textiles and silver nanowires. *J. Mater. Chem. C* **2019**, *7*, 9748–9755.

[17] Li, Q. S.; Chen, G.; Cui, Y. J.; Ji, S. B.; Liu, Z. Y.; Wan, C. J.; Liu, Y. P.; Lu, Y. H.; Wang, C. X.; Zhang, N. et al. Highly thermal-wet comfortable and conformal silk-based electrodes for on-skin sensors with sweat tolerance. *ACS Nano* **2021**, *15*, 9955–9966.

[18] Sun, B. H.; McCay, R. N.; Goswami, S.; Xu, Y. D.; Zhang, C.; Ling, Y.; Lin, J.; Yan, Z. Gas-permeable, multifunctional on-skin electronics based on laser-induced porous graphene and sugar-templated elastomer sponges. *Adv. Mater.* **2018**, *30*, 1804327.

[19] Li, Y. Y.; Wang, S. L.; Zhang, J. X.; Ma, X. H.; Cao, S. T.; Sun, Y. P.; Feng, S. X.; Fang, T.; Kong, D. S. A highly stretchable and permeable liquid metal micromesh conductor by physical deposition for epidermal electronics. *ACS Appl. Mater. Interfaces* **2022**, *14*, 13713–13721.

[20] Weng, W.; Chen, P. N.; He, S. S.; Sun, X. M.; Peng, H. S. Smart electronic textiles. *Angew. Chem., Int. Ed.* **2016**, *55*, 6140–6169.

[21] Ma, X. H.; Zhang, M. H.; Zhang, J. X.; Wang, S. L.; Cao, S. T.; Li, Y. Y.; Hu, G. H.; Kong, D. S. Highly permeable and ultrastretchable liquid metal micromesh for skin-attachable electronics. *ACS Mater. Lett.* **2022**, *4*, 634–641.

[22] Jin, H.; Matsuhisa, N.; Lee, S.; Abbas, M.; Yokota, T.; Someya, T. Enhancing the performance of stretchable conductors for e-textiles by controlled ink permeation. *Adv. Mater.* **2017**, *29*, 1605848.

[23] Kwon, C.; Seong, D.; Ha, J.; Chun, D.; Bae, J. H.; Yoon, K.; Lee, M.; Woo, J.; Won, C.; Lee, S. et al. Wearable electronics: Self-bondable and stretchable conductive composite fibers with spatially controlled percolated Ag nanoparticle networks: Novel integration strategy for wearable electronics (Adv. Funct. Mater. 49/2020). *Adv. Funct. Mater.* **2020**, *30*, 2070321.

[24] Fan, Y. J.; Yu, P. T.; Liang, F.; Li, X.; Li, H. Y.; Liu, L.; Cao, J. W.; Zhao, X. J.; Wang, Z. L.; Zhu, G. Highly conductive, stretchable, and breathable epidermal electrode based on hierarchically interactive nano-network. *Nanoscale* **2020**, *12*, 16053–16062.

[25] Jiang, Z.; Nayeem, O. G.; Fukuda, K.; Ding, S.; Jin, H.; Yokota, T.; Inoue, D.; Hashizume, D.; Someya, T. Highly stretchable metallic nanowire networks reinforced by the underlying randomly distributed elastic polymer nanofibers via interfacial adhesion improvement. *Adv. Mater.* **2019**, *31*, 1903446.

[26] Wu, Y. Y.; Mechael, S. S.; Lerma, C.; Carmichael, R. S.; Carmichael, T. B. Stretchable ultrasheer fabrics as semitransparent electrodes for wearable light-emitting e-textiles with changeable display patterns. *Matter* **2020**, *2*, 882–895.

[27] Li, Q. S.; Ding, C.; Yuan, W.; Xie, R. J.; Zhou, X. M.; Zhao, Y.; Yu, M.; Yang, Z. J.; Sun, J.; Tian, Q. et al. Highly stretchable and permeable conductors based on shrinkable electrospun fiber mats. *Adv. Fiber Mater.* **2021**, *3*, 302–311.

[28] Kim, D. H.; Lu, N. S.; Ma, R.; Kim, Y. S.; Kim, R. H.; Wang, S. D.; Wu, J.; Won, S. M.; Tao, H.; Islam, A. et al. Epidermal electronics. *Science* **2011**, *333*, 838–843.

[29] Cassidy, P. E.; Aminabhavi, T. M.; Thompson, C. M. Water permeation through elastomers and plastics. *Rubber Chem. Technol.* **1983**, *56*, 594–618.

[30] van Amerongen, G. J. The permeability of different rubbers to gases and its relation to diffusivity and solubility. *J. Appl. Phys.* **1946**, *17*, 972–985.

[31] Yang, X. Q.; Li, L. H.; Wang, S. Q.; Lu, Q. F.; Bai, Y. Y.; Sun, F. Q.; Li, T.; Li, Y.; Wang, Z. H.; Zhao, Y. Y. et al. Ultrathin, stretchable, and breathable epidermal electronics based on a facile bubble blowing method. *Adv. Electron. Mater.* **2020**, *6*, 2000306.

[32] Nawrocki, R. A.; Jin, H.; Lee, S.; Yokota, T.; Sekino, M.; Someya, T. Self-adhesive and ultra-conformable, sub-300 nm dry thin-film electrodes for surface monitoring of biopotentials. *Adv. Funct. Mater.* **2018**, *28*, 1803279.

[33] Zhao, Y.; Zhang, S.; Yu, T. H.; Zhang, Y.; Ye, G.; Cui, H.; He, C. J.; Jiang, W. C.; Zhai, Y.; Lu, C. M. et al. Ultra-conformal skin electrodes with synergistically enhanced conductivity for long-time and low-motion artifact epidermal electrophysiology. *Nat. Commun.* **2021**, *12*, 4880.

[34] Yeo, W. H.; Kim, Y. S.; Lee, J.; Ameen, A.; Shi, L. K.; Li, M.; Wang, S. D.; Ma, R.; Jin, S. H.; Kang, Z. et al. Multifunctional epidermal electronics printed directly onto the skin. *Adv. Mater.* **2013**, *25*, 2773–2778.

[35] Kabiri Ameri, S.; Ho, R.; Jang, H.; Tao, L.; Wang, Y. H.; Wang, L.; Schnyer, D. M.; Akinwande, D.; Lu, N. S. Graphene electronic tattoo sensors. *ACS Nano* **2017**, *11*, 7634–7641.

[36] Jang, K. I.; Chung, H. U.; Xu, S.; Lee, C. H.; Luan, H. W.; Jeong, J.; Cheng, H. Y.; Kim, G. T.; Han, S. Y.; Lee, J. W. et al. Soft network composite materials with deterministic and bio-inspired designs. *Nat. Commun.* **2015**, *6*, 6566.

[37] Jang, K. I.; Han, S. Y.; Xu, S.; Mathewson, K. E.; Zhang, Y. H.; Jeong, J. W.; Kim, G. T.; Webb, R. C.; Lee, J. W.; Dawidczyk, T. J. et al. Rugged and breathable forms of stretchable electronics with adherent composite substrates for transcutaneous monitoring. *Nat. Commun.* **2014**, *5*, 4779.

[38] Hsu, P. C.; Liu, X. G.; Liu, C.; Xie, X.; Lee, H. R.; Welch, A. J.; Zhao, T.; Cui, Y. Personal thermal management by metallic nanowire-coated textile. *Nano Lett.* **2015**, *15*, 365–371.

[39] Lee, Y.; Bae, S.; Hwang, B.; Schroeder, M.; Lee, Y.; Baik, S. Considerably improved water and oil washability of highly conductive stretchable fibers by chemical functionalization with fluorinated silane. *J. Mater. Chem. C* **2019**, *7*, 12297–12305.

[40] Zhou, Y. L.; Zhao, C. S.; Wang, J. C.; Li, Y. Z.; Li, C. X.; Zhu, H. Y.; Feng, S. X.; Cao, S. T.; Kong, D. S. Stretchable high-permittivity nanocomposites for epidermal alternating-current electroluminescent displays. *ACS Mater. Lett.* **2019**, *1*, 511–518.

[41] Tierney, T. B.; Rasmuson, Å. C.; Hudson, S. P. Size and shape control of micron-sized salicylic acid crystals during antisolvent crystallization. *Org. Process Res. Dev.* **2017**, *21*, 1732–1740.

[42] Chortos, A.; Koleilat, G. I.; Pfattner, R.; Kong, D. S.; Lin, P.; Nur, R.; Lei, T.; Wang, H. L.; Liu, N.; Lai, Y. C. et al. Mechanically durable and highly stretchable transistors employing carbon nanotube semiconductor and electrodes. *Adv. Mater.* **2016**, *28*, 4441–4448.

[43] Khan, U.; May, P.; Porwal, H.; Nawaz, K.; Coleman, J. N. Improved adhesive strength and toughness of polyvinyl acetate glue on addition of small quantities of graphene. *ACS Appl. Mater. Interfaces* **2013**, *5*, 1423–1428.

[44] Zhao, C. S.; Zhou, Y. L.; Gu, S. Q.; Cao, S. T.; Wang, J. C.; Zhang, M. H.; Wu, Y. Z.; Kong, D. S. Fully screen-printed, multicolor, and stretchable electroluminescent displays for epidermal electronics. *ACS Appl. Mater. Interfaces* **2020**, *12*, 47902–47910.

[45] Diridollou, S.; Patat, F.; Gens, F.; Vaillant, L.; Black, D.; Lagarde, J. M.; Gall, Y.; Berson, M. *In vivo* model of the mechanical properties of the human skin under suction. *Skin Res. Technol.* **2000**, *6*, 214–221.

[46] Lu, H. F.; Zhang, D.; Ren, X. G.; Liu, J.; Choy, W. C. H. Selective growth and integration of silver nanoparticles on silver nanowires at room conditions for transparent nano-network electrode. *ACS Nano* **2014**, *8*, 10980–10987.

[47] Liang, J. J.; Li, L.; Tong, K.; Ren, Z.; Hu, W.; Niu, X. H.; Chen, Y. S.; Pei, Q. B. Silver nanowire percolation network soldered with graphene oxide at room temperature and its application for fully

stretchable polymer light-emitting diodes. *ACS Nano* **2014**, *8*, 1590–1600.

[48] Song, T. B.; Chen, Y.; Chung, C. H.; Yang, Y.; Bob, B.; Duan, H. S.; Li, G.; Tu, K. N.; Huang, Y.; Yang, Y. Nanoscale joule heating and electromigration enhanced ripening of silver nanowire contacts. *ACS Nano* **2014**, *8*, 2804–2811.

[49] Lin, Y.; Li, Q. S.; Ding, C.; Wang, J. Y.; Yuan, W.; Liu, Z. Y.; Su, W. M.; Cui, Z. High-resolution and large-size stretchable electrodes based on patterned silver nanowires composites. *Nano Res.* **2022**, *15*, 4590–4598.

[50] Jeong, W.; Lee, S.; Yoo, S.; Park, S.; Choi, H.; Bae, J.; Lee, Y.; Woo, K.; Choi, J. H.; Lee, S. A hierarchical metal nanowire network structure for durable, cost-effective, stretchable, and breathable electronics. *ACS Appl. Mater. Interfaces* **2021**, *13*, 60425–60432.

[51] Zhou, Y. L.; Cao, S. T.; Wang, J.; Zhu, H. Y.; Wang, J. C.; Yang, S. N.; Wang, X.; Kong, D. S. Bright stretchable electroluminescent devices based on silver nanowire electrodes and high-k thermoplastic elastomers. *ACS Appl. Mater. Interfaces* **2018**, *10*, 44760–44767.

[52] Xu, B. X.; Akhtar, A.; Liu, Y. H.; Chen, H.; Yeo, W. H.; Park, S. I.; Boyce, B.; Kim, H.; Yu, J.; Lai, H. Y. et al. An epidermal stimulation and sensing platform for sensorimotor prosthetic control, management of lower back exertion, and electrical muscle activation. *Adv. Mater.* **2016**, *28*, 4462–4471.

[53] Kleiner, S. M. Water: An essential but overlooked nutrient. *J. Am. Diet. Assoc.* **1999**, *99*, 200–206.

[54] Hon, K. L. E.; Wong, K. Y.; Leung, T. F.; Chow, C. M.; Ng, P. C. Comparison of skin hydration evaluation sites and correlations among skin hydration, transepidermal water loss, SCORAD index, Nottingham Eczema Severity Score, and quality of life in patients with atopic dermatitis. *Am. J. Clin. Dermatol.* **2008**, *9*, 45–50.

[55] Yao, S. S.; Myers, A.; Malhotra, A.; Lin, F. Y.; Bozkurt, A.; Muth, J. F.; Zhu, Y. A wearable hydration sensor with conformal nanowire electrodes. *Adv. Healthc. Mater.* **2017**, *6*, 1601159.

[56] Hurley, M. V.; Bearne, L. M. Non-exercise physical therapies for musculoskeletal conditions. *Best Pract. Res. Clin. Rheumatol.* **2008**, *22*, 419–433.

[57] Lim, S.; Son, D.; Kim, J.; Lee, Y. B.; Song, J. K.; Choi, S.; Lee, D. J.; Kim, J. H.; Lee, M.; Hyeon, T. et al. Transparent and stretchable interactive human machine interface based on patterned graphene heterostructures. *Adv. Funct. Mater.* **2015**, *25*, 375–383.

[58] Sarzi-Puttini, P.; Cimmino, M. A.; Scarpa, R.; Caporali, R.; Parazzini, F.; Zaninelli, A.; Atzeni, F.; Canesi, B. Osteoarthritis: An overview of the disease and its treatment strategies. *Semin. Arthritis Rheum.* **2005**, *35*, 1–10.